Experimental study of the electric field in a hollow cathode discharge in hydrogen: influence of sputtering

V Gonzalez-Fernandez*[a], K Grützmacher[a], C Pérez[a] and M I de la Rosa[a]

[a] *Dpto. de Física Teórica, Atómica y Óptica, Universidad de Valladolid, Paseo Belén 7, 47011, Valladolid, Spain*

E-mail: veronica.gonzalez.fernandez@uva.es

ABSTRACT: Doppler-free two photon optogalvanic spectroscopy was employed in extensive studies to measure the electric field strength in the cathode fall region of a hollow cathode discharge (HCD), operated in pure hydrogen, via the Stark splitting of the 2S level of atomic hydrogen. The high quality measurements, based on an improved cathode design and laser spectroscopic set-up, reveal clear differences in the recorded spectra obtained for different cathode material (stainless steel and tungsten) at otherwise identical discharge conditions. It is well known, that the sputtering rate of tungsten is about four orders of magnitude less compared to stainless steel; hence the hydrogen plasma in front of the stainless steel cathode is much more contaminated by iron compared to tungsten. This study is focussed on analyzing the distortion of the spectra, i.e. the corresponding local electric field strength, depending on cathode material and laser power. We refer the more pronounced distortion of the spectra in case of a stainless steel cathode to the related large contamination of the hydrogen plasma due to atomic iron which is also expanding into the central discharge. Spectra recorded for different laser power, i.e. different spectral irradiance, allow verifying spectroscopic conditions, where the distortion of the spectra becomes quite negligible even for stainless steel cathode.

KEYWORDS: hydrogen plasma, sputtering, hollow cathode discharge, Plasma diagnostics - interferometry, spectroscopy and imaging, electric field strength, Stark effect

Contents

1. Introduction

Low densities hydrogen plasmas generated in different discharge devices have been investigated over several decades, experimentally and theoretically, [1-10]; and the references therein. Of particular interest is the profound understanding of the hydrogen plasma in the cathode fall region, because the local electric field strengths (E-field) in the cathode fall determines the fluxes of electrons and ions, their energies distribution and charge densities. Extensive studies i.e. [1,2,4] report on modelling of the collisional kinetics of pure hydrogen plasmas used to calculate among others the Hα-emission in order to characterize the cathode region of the plasmas, however precise direct measurements of the E-field are quite rare and extremely difficult.

Doppler free laser spectroscopy using optogalvanic detection has been demonstrated for the first time by us, to be well suited for E-field measurements in pure hydrogen and deuterium plasmas generated in a hollow cathode discharges, via the Stark splitting of the 2S level using tuneable single longitudinal mode (SLM) laser radiation [11,12]. As the E-field increases quite strongly in the cathode fall region (up to 4 kV/cm) a precise and independent determination of the spatial resolution provided by the laser spectroscopic condition was recently realized [13]. The unique experimental conditions, i.e. the SLM laser radiation with smooth temporal pulse shape, and the well-known cross sections for excitation, recombination and ionization of atomic hydrogen, open the possibility to determine the spatial resolution from first principles. It could be demonstrated an exceptional high spatial resolution: about 80% of the entire signal is created in a tiny measurement volume of 100 µm in diameter and 10 mm length; four times better than estimated before [11,12]. To maintain these conditions during an extended long lasting experimental measurement campaign, the laser-spectroscopic set up required a remarkably upgrade, as well as a continuous control of the laser irradiance present in the measurements volume to prevent signal saturation. Further effort was spent in a redesigned HCD. Substituting the usual hollow anode by a cone-shaped peaked anode improved the discharge symmetry and the short term stability of the discharge impedance, which is crucial for a stable background signal in optogalvanic detection. The HCD allows inserting hollow cathodes of different diameter and material: tungsten and stainless steel.

In a first measurement campaign we used tungsten cathodes, because tungsten has a minimal sputtering rate even in hydrogen discharges, in order to generate hydrogen plasma as clean as possible. The recently published results [14] revealed in fairly good approximation that the measured cathode fall characteristics do not depend on the cathode diameter of the HCD, and they are well suited therefore to be compared with experimental data - particularly - with data obtained from plane parallel electrode geometry [15-19]. Hence our results are valid to test one dimensional modelling of the cathode fall region of low pressure hydrogen discharge, and they may serve as reference measurements.

Stainless steel cathodes (cathode diameter of 10 mm and 15 mm) were employed in a second measurement campaign in order to see, how the HC hydrogen discharge would be affected by a remarkably larger sputtering rates: comparing the cathode fall characteristics with those obtained for tungsten cathodes. We expected that the differences in sputtering and the related contamination of the pure hydrogen plasma should show up in the cathode fall characteristics. Indeed the observed differences are found to be evident and extremely complex. The most unusual effect for the stainless steel cathode exhibited, that the E-field shifts remarkably to larger values with increasing laser power, which cannot be explained by usual signal saturation due to depletion of the ground state density of atomic hydrogen, increased photo ionization, etc. In this paper we give a brief overview of the experimental arrangement, and we present our first interpretation based on the differences of measured spectra of stainless steel and tungsten cathode while increasing the laser power.

2. Experimental arrangement and measurements

The experimental setup is the same used in ref [14], so here we only give the most important details. The Doppler-free measurements were performed with a tuneable laser in 243 nm, with a single longitudinal mode (SLM), 2.5 ns of temporal duration, up to 10 mJ pulse energy and a 300 MHz bandwidth. The counter-propagating beams were circularly polarized in opposite directions, so that only the simultaneous absorption of one photon of each beam provides two-photon excitation, according to the selection rules of the 1S-2S hydrogen transition ($\Delta L = 0$). The beams were focussed with lenses of 1 m focal length and overlapped in a 120 μm foci, which is controlled in situ with an UV camera. Regular measurements [14] were performed avoiding saturation [13] with 45 μJ pulse energy in each beam, corresponding to irradiance of about 150 MW/cm^2 in the overlap region. For each beam, the control of the pulse energy is provided by attenuators, rotating a $\lambda/2$ plate placed in front of a linear polarizer. These attenuators allow increasing the pulse energy up to 250 µJ, about five times more as commonly used, hence the dependence of recorded spectra on pulse energy.

The home-made HCD provides hydrogen discharges with excellent symmetry and long term and short term stability, and allows employing hollow cathodes of different inner diameters (10 and 15 mm) and materials (tungsten and stainless steel). The hollow cathode is placed between two anodes. The entire HCD is mounted on two translator stage, to perform precise vertical (y) and horizontal (x) displacements. The counter-propagating laser beams are crossing in the horizontal plane; and the measurement volume, i.e. the beam overlap, is aligned parallel to the cathode surface and centred with respect to the cathode length. The horizontal displacement guarantees the best alignment of the laser beams and the vertical allows performing measurements at different distances from the cathode surface. (see Fig. 1).

For the first study [14] tungsten cathodes have been used because of it well known low sputtering, and the measured E-field was very little affected when using twice the pulse energy.

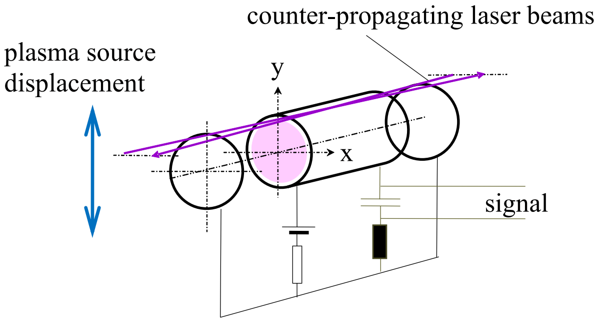

Figure 1: Scheme of the overlapping of the two laser beams. They are focalized in the upper-central part of the hollow cathode. This configuration allows Doppler-free measurements.

The spectra are recorded via optogalvanic detection, i.e. the signal is caused by resonant two-photon excitation and subsequent photo-ionization due to the absorption of a third laser photon. This increases the electron density in the tiny measurement volume, which can be detected as a transient variation of the discharge impedance between the cathode and one anode, via capacitive coupling.

To study the contamination of the hydrogen plasma due to cathode sputtering, we run the discharge with a stainless steel cathode. Stainless steel is a commonly used cathode material, having a sputtering rate of about 10^4 times larger compared to tungsten [20]. Therefore we expected some differences in the cathode fall characteristics, because sputtered iron is easily ionized by the laser radiation and an additional increase of charges particles in the measurement volume should show up in the measurements.

3. Influence of sputtering on cathode fall characteristics

Compared to previous cathode fall measurements [14] using tungsten cathode of 10 and 15 mm inner diameter we noticed some general differences operating the HCD with stainless steel cathode: in general, the optogalvanic signals were usually smaller for the stainless steel cathode and the background noise (peak to peak) was larger. However, the spectra varied extremely sensitive with respect to the pulse energy, never seen before for tungsten cathode discharge.

Fig 2 (a),(b) show two typical spectra - representing the Stark components of the 2S level - obtained for tungsten and stainless steel cathodes which demonstrate the differences of the dependence on pulse energy variation. We choose the same discharge current of 100 mA and a cathode diameter of 10 mm for the comparison, but different discharge pressures: 600 Pa for tungsten and 900 Pa for stainless steel. The corresponding E-fields are quite similar. For an easy comparison we only plot the corresponding fits of the measured spectra, see [14].

Fig 2 (a) shows the two spectra obtained for tungsten, one for low pulse energy of 45 μJ and a second recorded for twice the pulse energy. The corresponding E-fields are quite the same within an uncertainty of ± 2 %. The small differences in the widths of the Stark components are caused by a small saturation effect related to depletion of the atomic ground state density and to life time reduction of the 2S level due to increased photo-ionization.

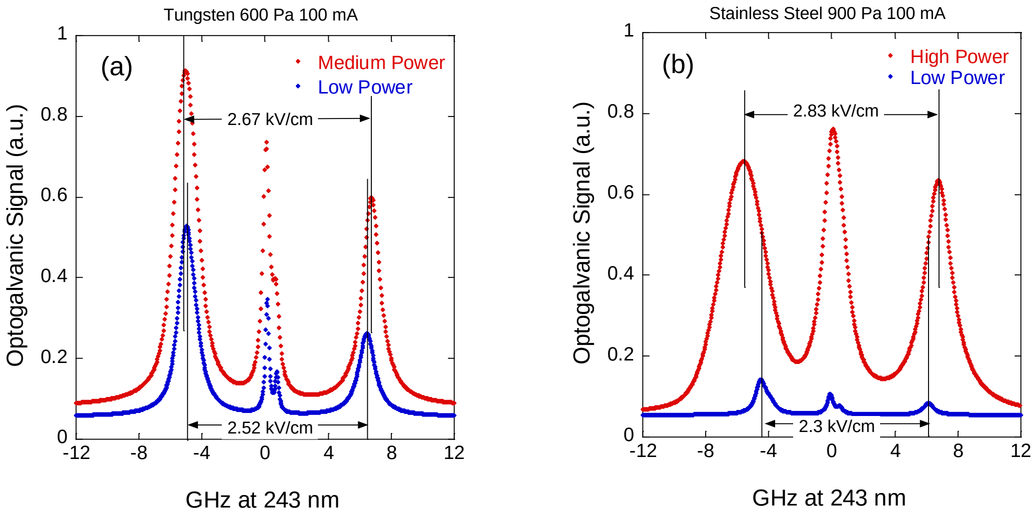

Figure 2: Comparison of spectra recorded at 160 μm from the cathode surface for different cathode material. (a) Tungsten cathode, 600 Pa, 100 mA. (b) Stainless steel cathode, 900 Pa, 100 mA**.**

An unusual distortion of the spectra (Fig 2 (b)) was observed for the stainless steel cathode while increasing laser power. In order to demonstrate this difference more pronounced, we show the spectra recorded for low pulse energy of 45 μJ and five times higher pulse energy. For the red and blue shifted Stark components we notice an additional anomalous shift towards larger E-field: from 2.3 kV/cm to 2.83 kV/cm, and an enormous broadening. Such differences cannot be explained by saturation effects due to depletion of in the atomic ground or life time reduction of the excited 2S level due to photo-ionization. These effects would cause only a broadening of the Stark components and only an insignificant increase of the E-field related to the underlying Stark effect.

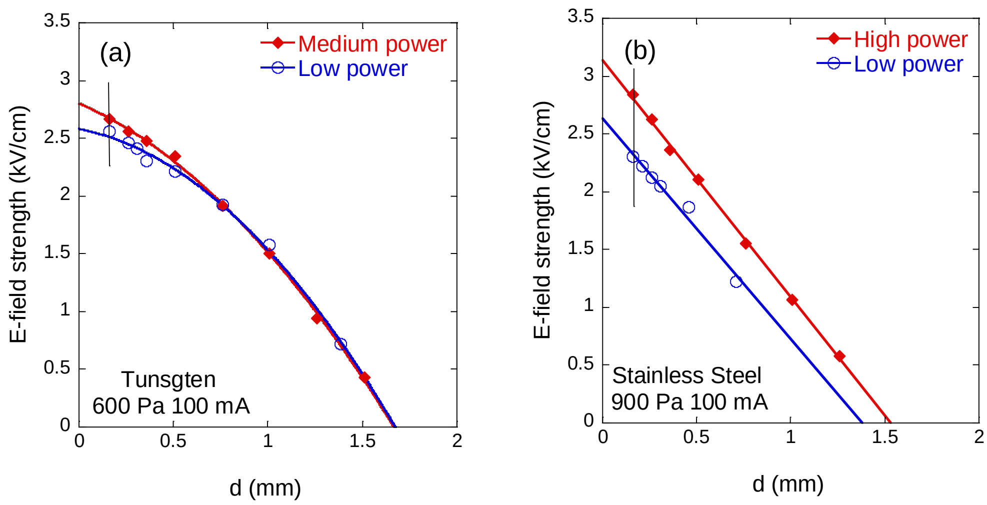

Figure 3: E-field strength vs. distance from the cathode surface for: a) tungsten and b) stainless steel cathodes, for different laser power. The vertical bars indicate the distance from the cathode surface of the spectra shown at figure 2.

Furthermore, Fig 3 (a) and (b) show the entire cathode fall characteristics for the corresponding discharge condition and pulse energies of Fig 2 (a) and (b). Obviously, for the tungsten cathode one observes some systematically and slightly larger E field close to the cathode surface only. For distances larger than 0.5 mm the measured E-field does not depend on the pulse energy variation. On the other hand, the E field for the stainless steel cathode is significantly larger for the entire cathode fall measured at higher pulse energies.

The reason for such phenomena may be referred to the different sputtering rates of tungsten and stainless steel, which is estimated to differ by 4 orders of magnitude [20]. The constant laminar hydrogen flow through the cathode region in the HCD corresponds to nearly zero gas flow velocity at the cathode surface and a parabolic increase of the velocity towards the maximum on axis. Therefore, in general the contamination of the pure hydrogen plasma due to sputtered material is larger close to the cathode surface and decreases toward the central plasma. The little difference in the cathode fall characteristics for tungsten is a clear indication of small contamination of sputtered material. In the case of stainless steel, pronounced differences exhibit, that the contamination is much larger, and that it expands into the entire cathode fall region.

Finally, Fig 4 (a) and (b) compares the cathode fall characteristic for tungsten and stainless steel, plotted for identical discharge conditions: 10 mm cathode diameter, 100 mA discharge current and two pressures of 600 Pa (a) and 900 Pa (b) measured with low pulse energy of 45 μJ. As can be seen, the E-field is always remarkably higher for the tungsten cathode compared to the stainless steel cathode. This confirms our previous conclusion, that the contamination of sputtered stainless steel is present in the entire cathode fall region. As atomic iron and the most dominant alloys of stainless steel as well have considerably lower ionization potential than hydrogen, the concentration of sputtered material increases the number density of charged particles, i.e. the conductivity of the plasma. Driving the same current density as in tungsten requires therefore less electric field. Presently we are studying in detail discharges in stainless steel cathodes of 10 and 15 mm diameter for a wide range of discharge conditions to be compared with the published data of tungsten [14].

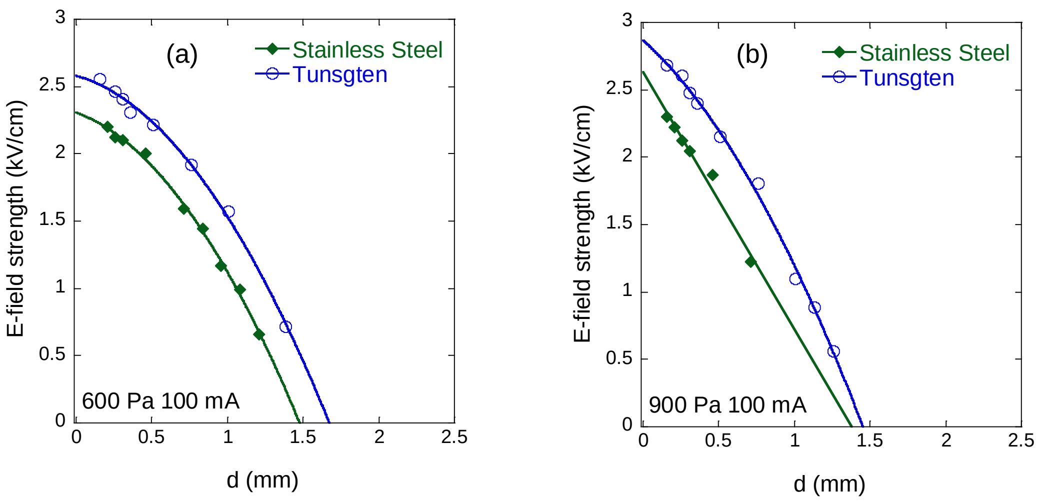

Figure 4: Comparison of the cathode falls for tungsten and stainless steel for two different pressures: 600 and 900 Pa, and a discharge current of 100 mA.

In order to fortify our conclusion, that the observed differences between tungsten and stainless steel are caused by sputtering, we analyze the influence of some other material parameters: the work function (external photo effect) of tungsten (5.2 eV) and stainless steel are similar because the most dominant alloys of stainless steel are iron (4.8 eV), chrome (4.5 eV) and nickel (5.3 eV). Therefore this reason can be excluded to cause the observed differences. This is also true for secondary electron emission due to positive hydrogen ion bombardment. From a study published in 1955 [21], we extract the secondary ion ratio being close to 1 for accelerator voltages below 20 keV. We also compare the difference of the inner cathode surface temperature T_c due to thermal conductivity. The heat conductivity for tungsten is about 170 W/mK but ten times smaller for stainless steel. For the conditions presented, we calculate a difference of 0.5 K between water cooled brass cathode holder and the cathode surface. For stainless steel, this difference amounts to about 5 K, which is also not relevant.

To summarise, it is important to keep laser energy under saturation levels. In tungsten cathodes exceeding the laser energy results in instability of the optogalvanic signal. However, in stainless steel cathodes, sputtered material is present in the whole discharge. This leads to a stable signal even with 5 times more energy than recommended, but the E-field results are not reflecting the unperturbed hydrogen discharge.

4. Conclusion

Doppler free laser-spectroscopy and optogalvanic detection is well suited to measure the local E-field strength in hydrogen discharges via the Stark splitting of the 1S-2S transition. In this paper HCD with two different cathode materials - tungsten and stainless steel - were employed to study contamination of the hydrogen plasma due to sputtered cathode material. Stark spectra recorded for laser pulse energy variation showed clear differences for tungsten and stainless steel cathode. Comparing the corresponding cathode fall characteristics, we concluded that the contamination of the hydrogen plasma is negligible for tungsten cathode, even close to the cathode surface. In the case of stainless steel we see evidence of contamination due to sputtering in the entire cathode fall. Nevertheless, the analysis also confirms that spectra recorded at low pulse energy of 45 μJ, i.e. irradiances not exceeding 150 MW/cm^2, are not perturbed at all by saturation effects, and provide therefore high precision E-field measurements and cathode fall characterisation.

Acknowledgments

The authors thank DGICYT (Ministerio de Economía y Competitividad) for the project ENE2012-35902, FEDER funds and the grants BES-2013-063248 and EEBB-I-16-10654 given to V. González-Fernández. The authors thank A. Martín and S. González for the technological support, J. L. Nieto for the informatics assistance, E. M. Domingo for the administrative work and A. Steiger for the scientific discussions.

References

[1] Phelps A V 2009 *Phys. Rev.* E **79** 066401

Phelps A V 2010 *Phys. Rev.* E **81** 029903

[2] Phelps A V 2011 *Plasma Sources Sci. Technol*. **20** 043011

[3] Jelenković B M and Phelps A V 1996 *Phys. Rev. E* **53** (2) 1852

[4] Jelenković B M and Phelps A V 2011 *Phys. Plasmas* **18** 103505

[5] Gemisic Adamov M, Obradovic B M, Kuraica M M and Konjević N 2003 *IEEE Transactions on Plasma Science,* **31** (3) 444-454.

[6] Gemisic Adamov M, Steiger A, Grützmacher K and Seidel J 2007 *Phys. Rev. A* **75** 013409

[7] Spasojević D J, Steflekova V, Šišović N M and Konjević N 2012 *Plasma Sources Sci. Technol.* **21** (2) 025006

[8] Spasojević D J, Steflekova V, Šišović N M and Konjević N 2014 *Plasma Sources Sci. Technol.* **23** (1) 012004

[9] Spasojević D J, Mijin S, Šišović N M and Konjević N 2016 *J. Appl. Phys*. **119**, 053301

[10] Jiménez-Redondo M, Carrasco E, Herrero V J and Tanarro I 2015 *Plasma Sources Sci. Technol.* **24** 015029

[11] de la Rosa M I, Pérez C, Grützmacher K and Fuentes L M 2009 *Plasma Sources Sci. Technol.* **18** 015012

[12] Pérez C, de la Rosa M I and Grützmacher K 2010 *Eur. Phys. J. D.* **56** 369-375

[13] García-Lechuga M, Fuentes M, Grützmacher K, Pérez C and de la Rosa M I 2014 *J. Appl. Phys.* **116** 133103

[14] Gonzalez-Fernandez V, Grützmacher K, Steiger A, Pérez C and de la Rosa M I 2017 *Plasma Sources Sci. Technol* **26** 105004

[15] Güntherschulze A 1928 *Z. Phys*. **49** 473

[16] Güntherschulze A 1930 *Zeitschrift für Physik A Hadrons and Nuclei* **59** (7) 433-445

[17] Warren R 1955 *Phys. Rev*. **98** 1650

[18] Barbeau C and Jolly J 1990 *Appl. Phys. Lett.* **58** 237

[19] Cvetanović N, Kuraica M M and Konjević N 2005 *J. Appl. Phys.* **97** 033302

[20] Matsunami N, Yamamura Y, Itikawa Y, Itoh N, Kazumata Y, Miyagawa S, Morita K, Shimizu R and Tawara H 1984 *At. Data Nucl. Data Tables* **31**, 1-80

[21] Murdock J W, and Miller, G H 1955 United States Atomic Energy Comission Report: *Secondary electron emission due to positive ion bombardment*